EUROVOLC

European Network of
Observatories and Research Infrastructure for Volcanology

Deliverable Report

Deliverable 10.2 - Joint modelling of monitoring data sets

Work Package:	*Integration and modelling of geophysical, geochemical and petrological monitoring data*	
Work Package number:	10	
Work Package leader:	*Andy Hooper*	
Task (Activity) name:	*Integrated Modelling of Monitoring Data*	
Task number:	*10.1*	
Responsible Activity leader:	*Andy Hooper*	
Lead beneficiary:	*UNIVLEEDS*	
Author(s)	*François Beauducel, Maria Angeles Benito-Saz, Valerie Cayol, Elena Gonzalez, Andy Hooper, Daniel Juncu, Benedikt Ófeigsson, Michelle Parks, Aline Peltier, Melissa Pfeffer, Freysteinn Sigmundsson.*	
Type of Deliverable:	*Report [X]* *Prototype [ ]*	*Demonstrator [ ]* *Other [ ]*
Dissemination level:	*Public [X]* *Prog. Participants [ ]*	*Restricted Designated Group [ ]* *Confidential (consortium) [ ]*

Programme: H2020
Project number: 731070

Table of Contents

Summary

The description for this deliverable is “Monitoring of subsurface magma movements and dynamics through automated joint modelling of multiple data sets, including guidelines for best practice.” Typically, different types of monitoring data set are interpreted individually, rather than together and this deliverable represents an ambitious target to not only develop new approaches for joint inversion, but to also make them fully automated. What we have achieved is to develop four different approaches to joint modelling/interpretation of multiple data sets, but none of these is yet mature enough to implement in an automated way. On the other hand, we have made significant progress in automating the detection of new deformation and changes in the rate of background deformation at volcanoes, using InSAR data. These results can be visualised along with an automated system for visualising other monitoring data that we previously developed, allowing joint interpretation by observatories.

We have also developed guidelines on best practice for monitoring volcanoes using automatic systems only, i.e., without field investigations. This is important when scientists and technicians are unable to go into the field, such as occurred during the global pandemic, and also for volcanoes that lack a local observatory. These guidelines emphasise 1) the importance of using both remote-sensing data and ground-based instrumentation, 2) the need for a ground-based network of sufficient density such that no individual instrument is critical to the monitoring, and 3) the necessity of a redundant communication system for relaying data from the ground-based instruments.

Introduction

Various different types of data, such as seismic, geodetic and volatile emission/geochemical data, can be gathered during volcanic crises for monitoring purposes. Typically, different types of data are processed separately, but modelling of these data jointly can lead to a more consistent understanding. To better interpret all three data types rapidly and in a joined-up manner, we have investigated three different approaches for interpreting the data separately and together in near real time, depending on what data are available: 1) integration of InSAR/GNSS, and gas measurements; 2) integration of InSAR and gas remote sensing data; 3) integration of InSAR/GNSS, seismology and petrology. In addition, we have developed an approach to modelling geodetic data that allows for the integration of other data sets that illuminate the location of subsurface sources, such as magnetotelluric data. The details of each approach are provided in the following sections.

1. Integration of InSAR/GNSS, and gas measurements

On the 21st January 2020, the Svartsengi/Eldvörp volcanic system located on the Reykjanes Peninsula reactivated, characterized by seismic swarms and high-rate deformation. This activity is believed to be triggered by magma migration at depth beneath a large section of the Reykjanes Peninsula, resulting in three detected magmatic intrusions in the vicinity of Mt Þorbjörn and an additional intrusion near Krýsuvík. The last eruptive activity in this area was approximately 800 years ago (1235 Illahraun, Arnarseturshraun and Eldvarpahraun lava flows), with a suggested inter-rifting interval on the Reykjanes Peninsula of around 600-1000 years (Sæmundsson et al., 2020). These were effusive (lava forming) eruptions where activity comprised lava fountaining and the extrusion of basaltic lava flows. Historic eruptions have formed crater rows, comprising up to 100 craters. At the onset of these types of eruptions, the entire length of the fissure is initially active (length ~10 km), then as the eruption progresses activity will become focused on parts of the fissure or individual craters.

InSAR analysis was undertaken using the Stamps Persistent Scatterers technique (Hooper et al., 2007) to map the line-of-sight (los) deformation associated with the intrusions in the vicinity of Mt. Þorbjörn. The average velocity map, utilizing data from Sentinel-1 track 16 is displayed in Figure 1 and the los time-series extracted from the centre of deformation in Figure 2. The three intrusions (periods of uplift) occurred between: 1) 21st January-6th February; 2) 6th March-17th April; and 3) 15th May-22nd July.

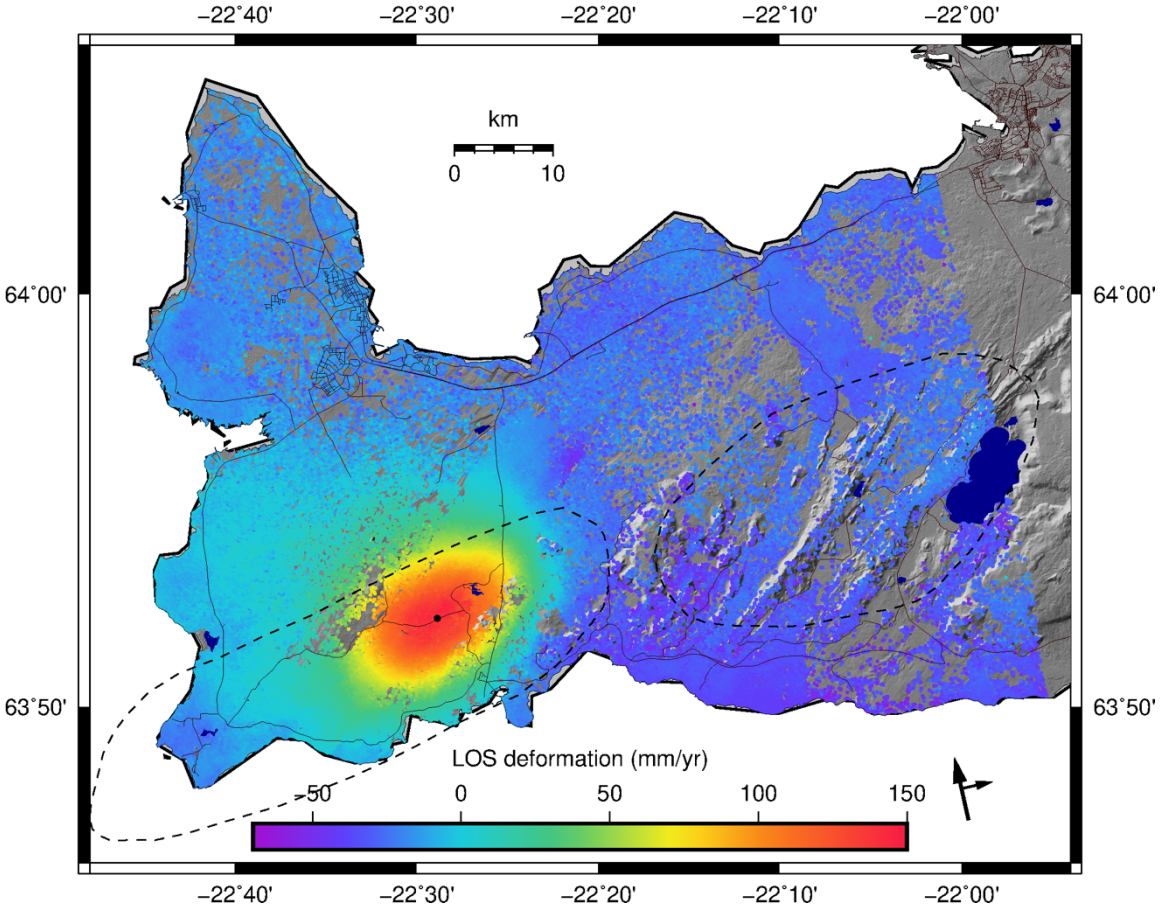

Figure 1. Average line-of-sight (los) velocity map for the Reykjanes Peninsula, covering the period 20th January 2020 to 24th July 2020, utilizing satellite data acquired by Sentinel-1 track 16. Red amplitudes represent region of inflation as a result of three separate magmatic intrusions occurring between: 1) 21st January-6th February; 2) 6th March-17th April; and 3) 15th May-22nd July.

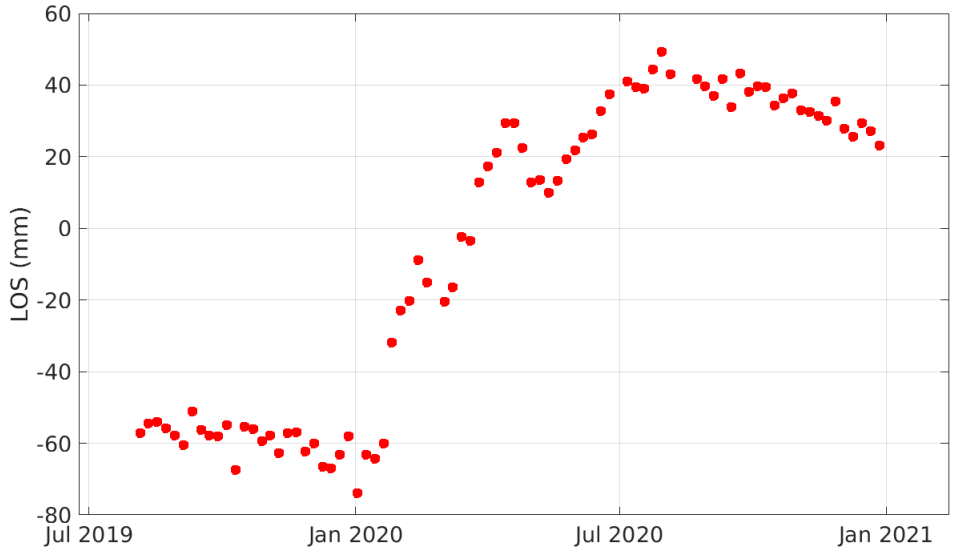

Figure 2. Time-series of line-of-sight (los) deformation for the Reykjanes Peninsula, utilizing satellite data acquired by Sentinel-1 track 16. The time-series is extracted from the reference point (black circle) displayed in Figure 1.

A combination of GNSS and InSAR observations have been used as an input into geodetic inversions to determine the best-fit source parameters for the observed deformation. The results suggest three near-horizontal, elongated magmatic intrusions have been emplaced in the vicinity of Mt Þorbjörn since the onset of the unrest (Figure 3), situated at a depth of approximately 4 km beneath the surface.

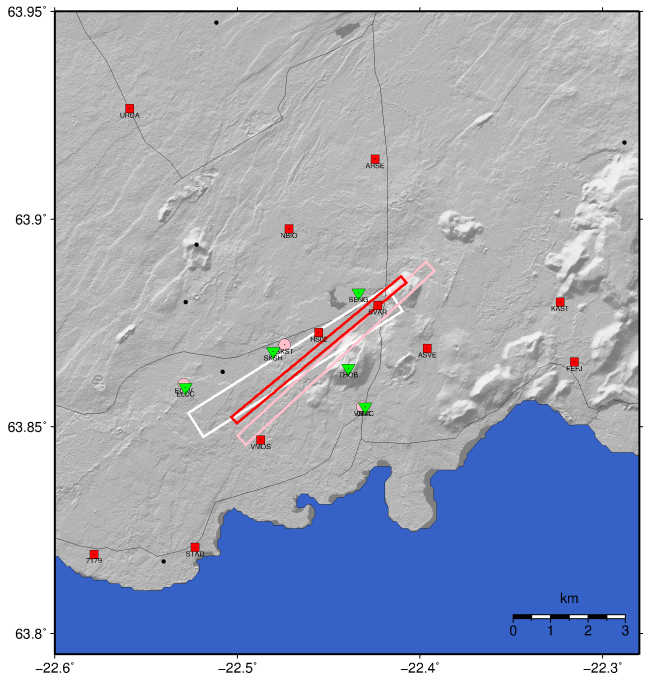

Figure 3. Location of magmatic intrusions (rectangles) in the vicinity of Mt Þorbjörn. Continuous GPS stations are displayed as green triangles, campaign GPS stations as red squares and seismic stations as pink circles.

As reported in M1-18, a joint visualization tool representing real-time monitoring data for seismic, GNSS, gas and hydrological data at Katla Volcano has been implemented and has been in operation for some time. A further development of the tool includes a draft of a command line program and a config structure which uses the three components of the program to retrieve, analyze and view the data defined by criteria such as geographical boundaries, data types, station list and is intended to simplify the integration of this tool to different areas with different monitoring needs. An example of this monitoring plot, incorporating data acquired throughout the recent unrest on Reykjanes peninsula is displayed in Figure 4. At present, this only includes seismicity and GNSS data, as gas measurements in this area to date have only been undertaken during campaign (point) surveys and no continuous measurements are available yet. These can however be added once a permanent continuous station has been established.

The tool is comprised of three independent components. Data import: where data is read in from the particular institution's archives (IMO in this case) - this will require modification dependent on the variable data structures of different institutions, however it will output the data in a standard format necessary for the other components to be able to work. Data analyses: this component can be used to process, further analyse and model the data, here the integrated modelling of monitoring data (10.1.2) can be implemented and visualized by the third component. Visualization: this component plots and visualizes the data and/or relevant models derived from it. Currently, only the data is displayed using this tool however it is anticipated that models derived from the data can also be added to the figures. The tool is written in python and makes use of the numerical packages numpy and pandas. Further development is currently underway to add a map view of the time series data.

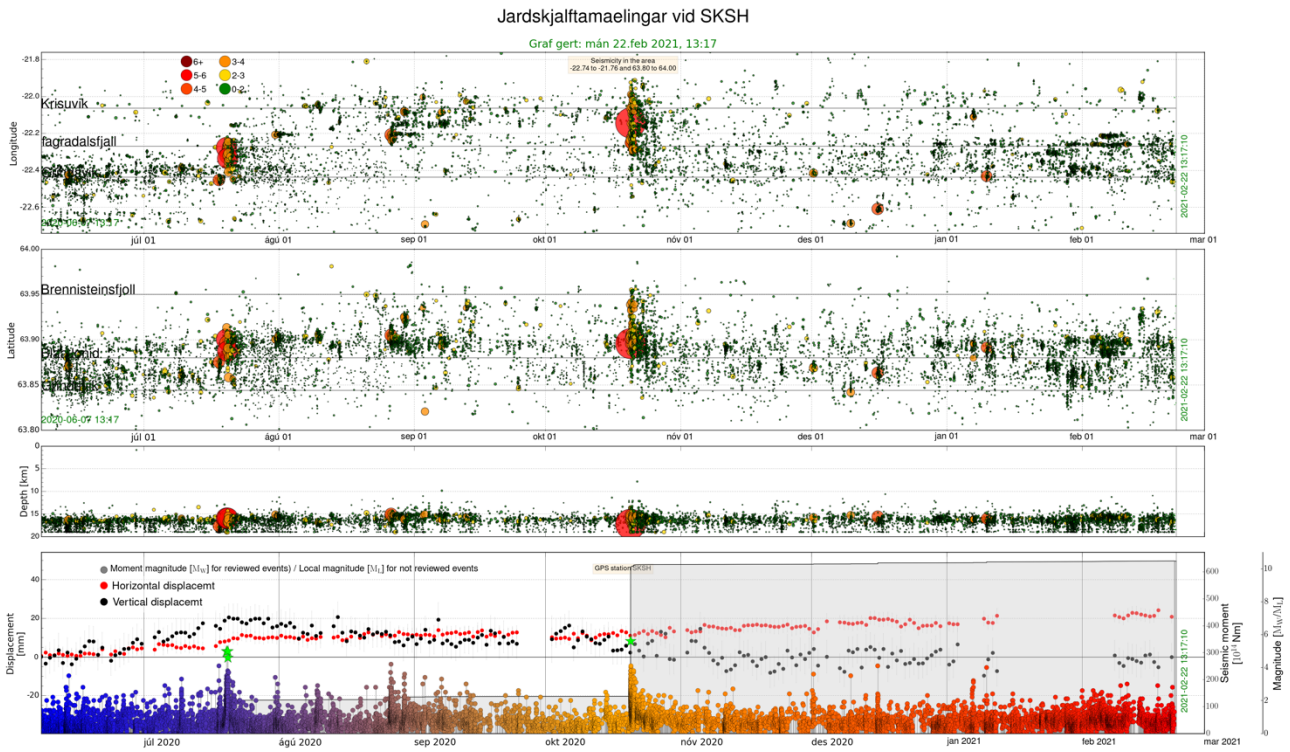

Figure 4. Muliplot display for Reykjanes Peninsula, incorporating seismicity and GNSS data for station SKSH.

Campaign style gas measurements in this area commenced on the 12th February 2020 and have continued throughout this ongoing episode of unrest. These comprised multi-gas measurements (CO_2, SO_2, H_2S and H_2) and radon measurements at two sites with surface gas emissions (close to Svartsengi geothermal borehole SV10 and Eldvörp). Initial results indicate a correlation between radon emissions at site SV10 and seismicity in the Þorbjörn area during the second intrusive period (6 March-17 April, 2020, Figure 5). This period corresponds to the largest increase in seismic moment (larger magnitude earthquakes occurred during this period).

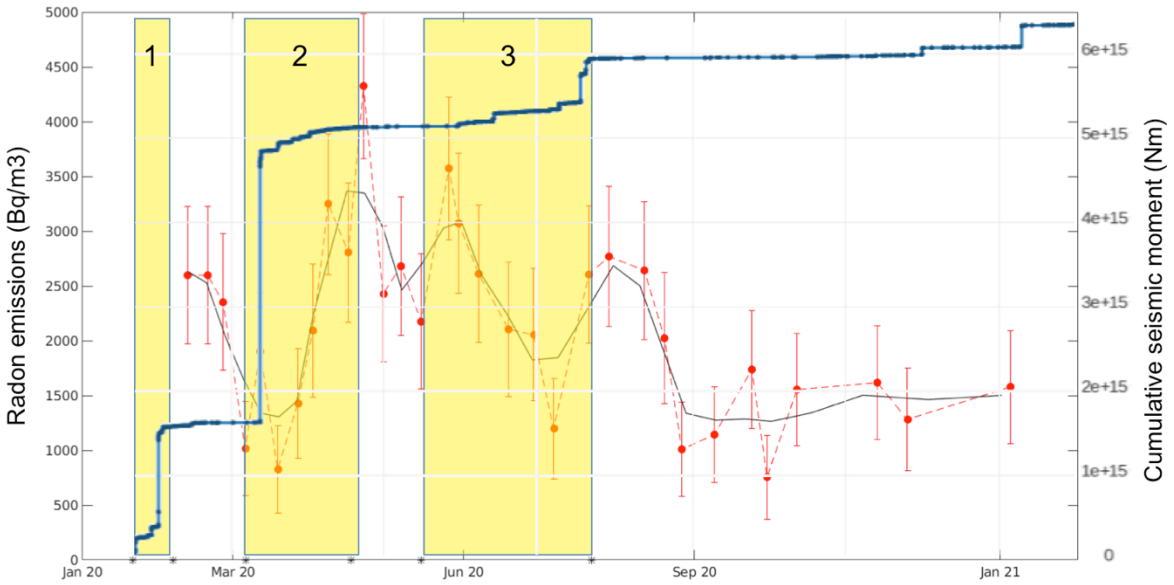

Figure 5. Correlation between seismicity and radon emissions at site SV10. Yellow boxes mark the three separate intrusive periods. Red dots represent the average radon emissions with associated error bars. The grey curve displays the filtered results. The blue line represents the cumulative seismic moment.

We aim to use geodetic, seismic and gas observations made during this recent unrest to constrain multi-parameter models of the sub-surface plumbing system and magma migration pathways. At present only campaign style point measurements have been undertaken to monitor the gas emissions. Although there appears to be a correlation between magmatic and seismic activity and radon emissions, ideally, continuous real-time radon measurements should be undertaken to validate this relationship and aid with near-real-time forecasting. A new radon detector has been developed at the German Research Centre for Geosciences (GFZ) specifically designed for long-term, continuous measurements of radon emissions. We plan to install this equipment at a designated site at Svartsengi to investigate the feasibility of using a time-series of radon observations combined with seismic and deformation measurements in Iceland for forecasting changes in volcanic behavior, as has been done in other volcanic areas (e.g. after Heiligmann et al., 1997 and Padilla et al., 2013).

2. Integration of InSAR and gas remote sensing data

UCA have developed an approach for jointly inverting ground displacements from InSAR and gas remote sensing data, which they applied to the 2015 eruption of Ambrym volcano (Shreve et al., 2021). In this approach, ground displacements are inverted to determine the geometry and volume change of a subsurface reservoir. For Ambrym, UCA showed that a dike and reservoir interacted with a caldera bounding fault. Using reasonable bounds on pressure change, the magma compressibility can then be estimated. Independently, volumes of emitted SO_2 are used to estimate

the reservoir volume. This volume, together with the compressibility and the pressure change in the reservoir leads to constraints on the amount of magma extracted. In the case of Ambrym, UCA estimated that only 2-6% of magma was extracted from the reservoir before caldera ring fault failure. This suggests that caldera formation may form by hundreds of subsidence episodes no greater than a few meters.

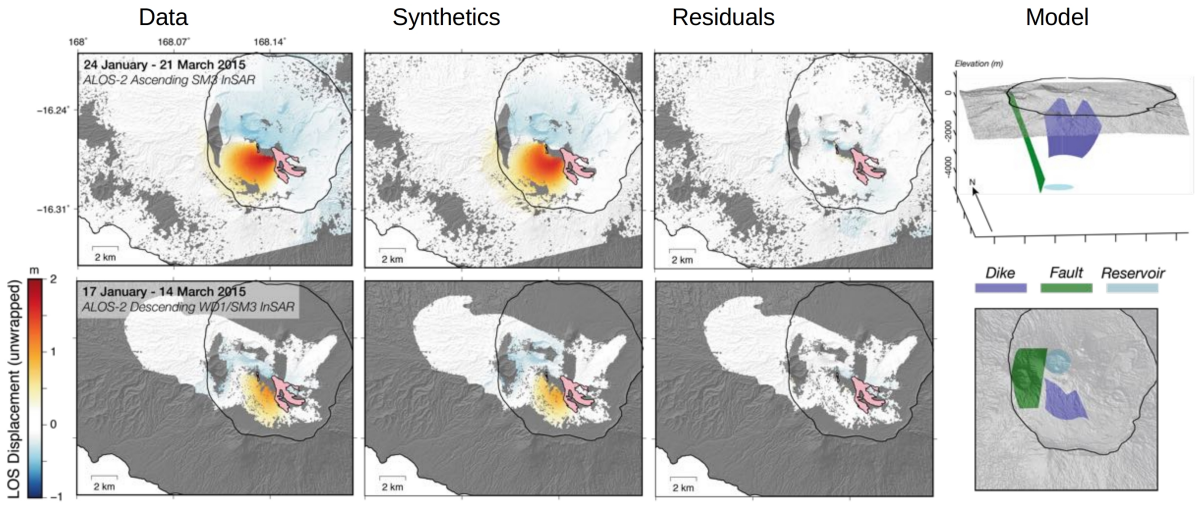

Figure 6: Data, Synthetics, residuals and best model for the Ambrym 2015 eruption. Three sources (a dyke, a fault and a reservoir) are required to fit the ground displacements.

3. Integration of InSAR/GNSS, seismology and petrology

UI together with IMO and UNIVLEEDS have developed a new framework for joint modelling of the monitoring data sets, considering magma ascent processes, magma chamber dynamics and the stress field of volcanic systems. The approach has been published in a recent paper in Nature Communications (Sigmundsson et al., 2020). The study sheds light on what conditions need to be in place in a volcano for an eruption to start, and furthermore how eruptions develop and lead to caldera formation, i.e. when a large part of a volcano subsides at the same time as a large amount of magma reaches the surface, as was the case in the 2014-2015 Bárðarbunga activity in Iceland.

Previous methods to understand magma movements in the surface have certain limitations and are based on assumptions that are not always applicable. It is also noteworthy that some large-volume eruptions have small or minor precursors in terms of increased earthquake activity and magma movements. Small eruptions can on the other hand have large precursors. This is not what is expected from commonly used models that volcanologists have used to interpret monitoring data from volcanoes. Within EUROVOLC, a new method was developed to take jointly into consideration three important effects that influence how magma accumulates and then forces its way to the surface.

Firstly, magma may be less dense than the host rock surrounding it. Where magma accumulates in volcano roots it can therefore have a large upward directed buoyancy force (Fig. 7). This means that if sufficient magma accumulates, this force alone can break the surrounding host rock and magma can flow upwards.

Secondly, the host rock around magma bodies in volcano roots can behave as a ductile material. It can deform and flow in a "viscoelastic manner" – such that solid rocks yields away from the magma and creates space for new magma without fracturing. This can happen if magma accumulates over long time, many years or still longer time periods.

Finally, it must be considered that magma can form pipe-like pathways e.g. by eroding away part of surrounding rocks where magma flows. Such sustained magma channels do not easily close, even if pressure drops in underlying magma bodies that feed these magma channels. This means that following the peak of an eruption such a channel can thus remain open for considerable time.

By connecting these three factors together into one methodology a new approach to understand magma movements was created.

The method was then by applied to data gathered in the time leading up to the test case of Bárðarbunga 2014-2015 events in Iceland, to demonstrate its applicability. The series of events observed at Bárðarbunga can be explained by the existence of magma below Bárðabunga for a long time prior to the eruption. The rock surrounding the magma yielded creating space for the magma. Evaluation of the magma and rock's density shows that the magma could easily flow upwards. The magma was thus almost ready to burst forward, needing only a small inflow of additional magma to start the eruption. Thus, a sustained magma channel was formed from the magma accumulation area resulting in a large drop in pressure leading to the caldera formation in Bárðarbunga.

The results are important as the method developed can be applied to all volcanoes. The method points to certain features that scientists and those who monitor volcanoes need to consider when estimating if a new eruption will begin. Large eruptions can occur with only minor precursory activity.

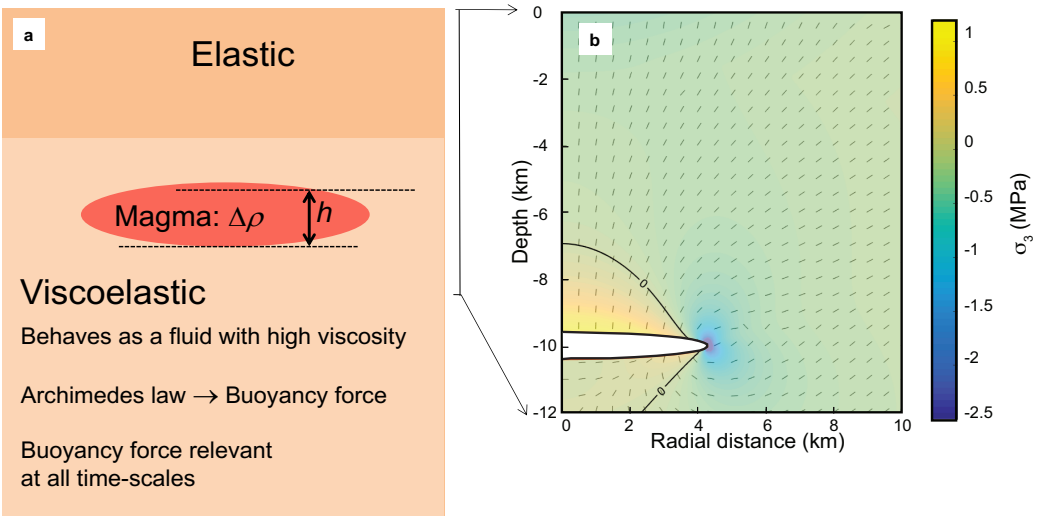

Figure 7. Model and stress field due to buoyancy. (a) Schematic model of a magma body residing in viscoelastic material below an elastic layer. The magma is less dense than the host rock and therefore buoyant. The density difference between magma and host rock is $\Delta\rho$, and h is the elevation above the bottom of the magma body. (b) Stress due to buoyancy around a horizontal ellipsoid, with a 4.3 km semi-major axis and a 0.4 km semi-minor axis, embedded in an elastic medium with a Poisson's ratio of 0.25. The density contrast is set to 270 kg/m^3. Pressure equal to $\Delta\rho gh$, with g being the acceleration of gravity, is applied at its boundary. The colour scale shows the amplitude of the minimum compressive stress (negative values for tension) and dashes represent the direction of maximum compressive stress (σ_1). The crustal volume immediately above the magma body is under compression, but the edge of the body is affected by a large tensile stress allowing for dike initiation. Above the body, the stress field is similar to the one induced by overpressure resulting from magma inflow.

4. Integration of InSAR and magnetotelluric data

Magnetotelluric (MT) surveys provide extra constraints on source of deformation and allow for quantification of source processes (e.g., degassing). To incorporate these constraints in inversion of deformation data, UNIVLEEDS have developed a code (https://github.com/djuncu/GEDI) to invert one or more InSAR datasets for distributed subsurface volume change, following the approach laid out by Vasco et al. (1988, 2000) and Mossop & Segall (1999). The model consists of a fixed grid of subsurface cells whose deformation can be linked to displacements of points at the surface through a set of Green's functions. By using (InSAR) observations of surface displacements, and as long as the subsurface grid is fixed, this becomes a linear inverse problem that can be solved for individual volume change of each grid cell. The code solves the linear inverse problem using singular value decomposition. We found that regularization as well as a non-negative inversion approach are required to stabilize the results. The code incorporates downsampling of the InSAR data using a quadtree approach. Topography effects are integrated in a simple, first-order way, by taking varying elevation into account when calculating the distance between surface points and subsurface grid cells.

While the rather large number of degrees of freedom using this approach makes it difficult to resolve the true depth of deformation (due to source-strength / depth ambiguity) from deformation data alone, it can be readily combined with constraints on source position from MT data, which serve to regularise the inversion.

Automation

The four approaches outlined above are different methods for jointly interpreting multiple monitoring data sets. Although these represent significant progress in the direction of joint interpretation, these approaches are still in the development stage are not yet mature enough to be implemented in an automated way.

Where we have made progress, in terms of automation, is in the detection of new deformation sources, and changes in the rate of existing deformation sources. The foundation for this approach is described in Deliverable Report D9.2 and Gaddes et al. (2019). The threefold approach consists of 1) isolating signals of geophysical interest from interferograms using independent component analysis (ICA), 2) using the components learned in stage 1 to characterise the baseline data and 3) ingestion of new interferograms to determine whether the signals present have deviated strongly enough from those in the baseline data to warrant flagging the volcano as having entered a period of unrest. The algorithm was tested on synthetic datasets as well as real data from the Sierra Negra volcano (Galapagos, Ecuador).

UNIVLEEDS have further developed this technique to a state of full automation. This has involved development of an automated time series algorithm (LiCSBAS; Morishita et al, 2020), which takes interferograms generated by the LiCSAR system (Lazecky et al, 2020) and outputs times series of displacements for individual pixels. A series of scripts have been written that now run LiCSBAS automatically on a list of 250 volcanoes judged to be the most likely to have an impact, based on likelihood of eruption and the risk to populations. The ICA approach of Gaddes et al. (2019) has been further developed to improve sensitivity for volcanoes that are deforming at a low rate and to run in an automated way without any manual intervention. An example of the output generated is shown in Figure 8. LiCSAlert is now running on the 250 high-priority volcanoes, with the intention to roll out to all volcanoes globally as the next step.

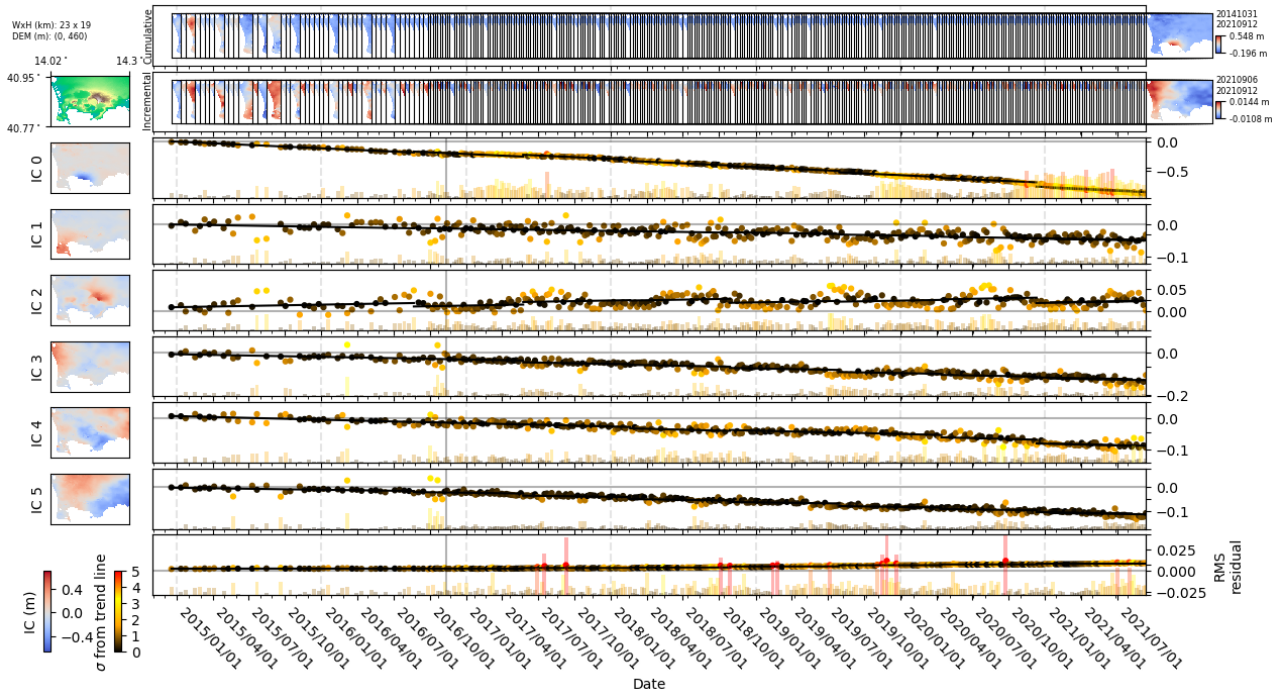

Figure 8. LiCSAlert output snapshot for Campi Flegrei (updated every six days). The six independent components, representing background signals present in the time series of interferograms for the first two years, are shown on the left (IC 0 to IC 5). The cumulative contribution of each IC to every interferogram (each spanning six days) is shown to the right of each IC. IC 0 represents the background subsidence signal, and a slight acceleration from Nov 2020 is flagged by the yellow and red bars, which indicate a stronger than usual contribution. IC 2 represents the hydrostatic part of the tropospheric signal, and its contribution fluctuates seasonally. The other ICs represent atmospheric conditions that are prevalent in the time series of interferograms.

Although we have not yet reached the ambitious goal of automated joint modelling of multiple data sets, LiCSAlert output can be displayed alongside the joint visualisation tool delivered in D10.1, which adds to the ability to jointly interpret multiple data sets. The independent components and residuals also provide useful inputs into the joint inversion methods that are still being developed as described above.

Best Practice

We are not yet in a position to consider best practice in terms of automated joint inversion, due to the lack of maturity of the approaches we have developed. The global pandemic did, however, lead to the chance to consider best practice for using multiple automated data streams to monitor eruptions, when no field investigation is possible. An eruption of Piton de la Fournaise in April 2020 provided the test case.

Remote volcanic crisis management is particularly important not only at volcanoes lacking an observatory, but also at well-equipped volcanoes in which access is temporarily hampered or disabled. Such factors include, for example, cyclones and blizzards, or national strikes, civil disorder, wars, or pandemics. IPGP showed how it was important to have both field ground stations and remote sensing data, especially when no field investigation is possible (Peltier et al., 2020). In March 2020, the coronavirus disease 2019 outbreak was declared a pandemic by the World Health Organization and became a global health crisis. Authorities worldwide implemented lockdowns to

restrict travel and social exchanges in a global effort to counter the pandemic. In France, and in French overseas departments, the lockdown was effective from 17 March to 11 May 2020. It was in this context that the 2–6 April 2020 eruption of Piton de la Fournaise (La Réunion Island, Indian Ocean) took place. The density and reliability of the observatory networks (seismometers, GNSS, tiltmeter, extensometer, gas stations), combined with satellite observations, allowed for trustworthy instrument-based monitoring of the eruption (Figure 9) and continuity of the observatory duties in issuing regular updates of volcanic activity in the context of a double crisis: volcanic and health.

Guidelines on best practice for monitoring using automated data streams without field investigations are as follows:

1. It is important to have both remote-sensing and ground-based measurements. For the April 2020 eruption, the displacement pattern mapped using SAR interferometry was rather weak in magnitude and limited to the immediate surroundings of the eruptive vent. No GNSS station was located within this displacement pattern. Hence, without satellite observations, this displacement would have been completely unnoticed. Vice versa, the pre-eruptive inflation in the four days prior to the eruption recorded by the GNSS stations was too weak to be detected by InSAR.

2. A dense, resilient monitoring network must be installation and tested prior to a crisis, such that any individual station is not critical to be able to monitor the activity. As shown for the April 2020 eruption, the loss of one station was not critical for efficient monitoring, as a functioning network of a sufficiently dense instrument array was in place. Even changes in eruptive activity, such as the paroxysmal activity toward the end of the eruption, could be recognized and followed despite the loss of the nearest monitoring station

3. Data transmission relays need to be designed with in-built redundancy. For example, on 31 December 2005 (during an eruption), heavy thunderstorms damaged a transmission relay and data were no longer transmitted to observatory. The observatory staff were therefore blind to what was happening on the ground for a few hours while the situation was being repaired. Since that time, the observatory has developed several, partially redundant relays, so that data pass through different relays, and in the case of failure of one data reception is still assured.

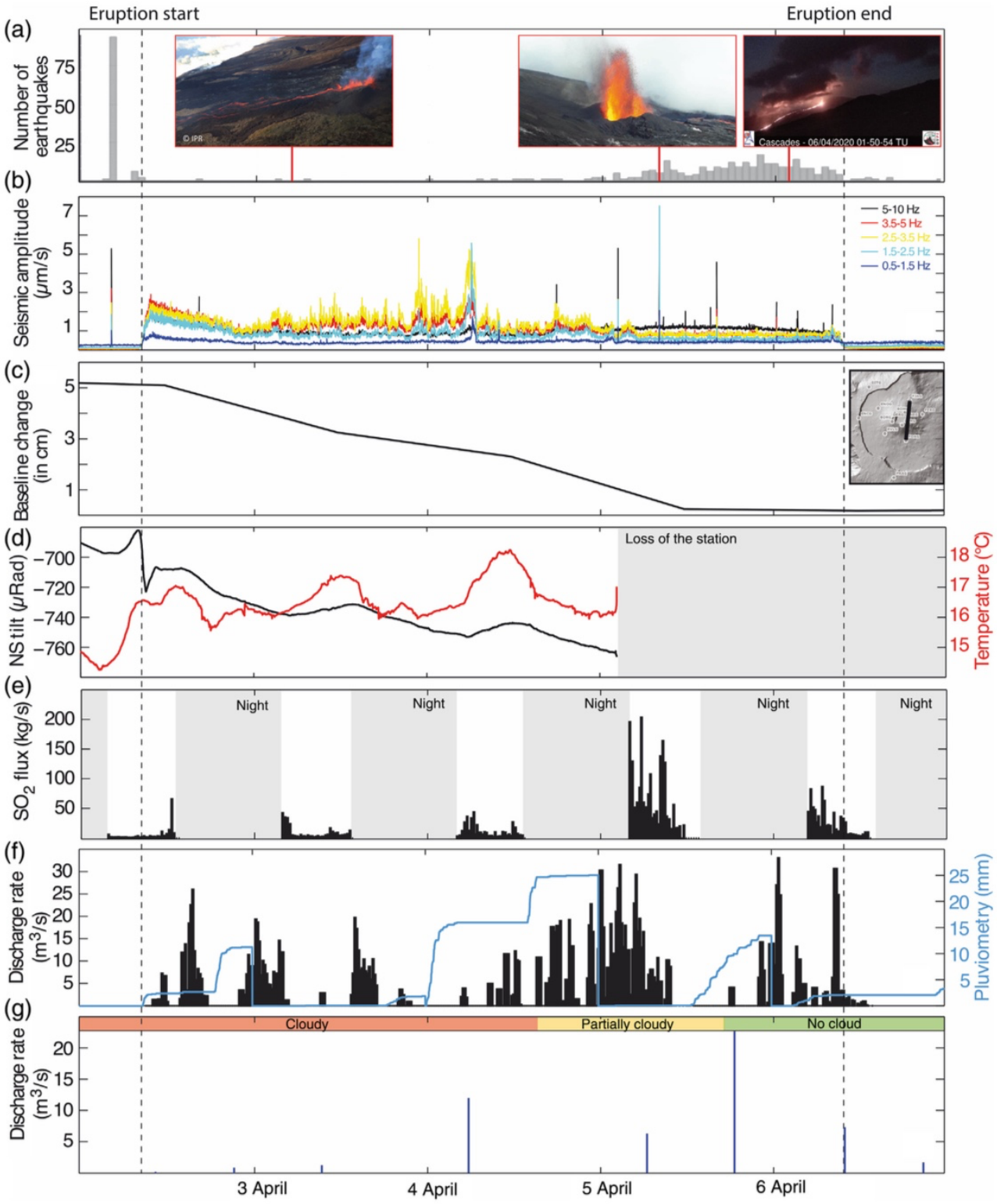

Figure 9 : Geophysical and geochemical trends during the 2–6 April 2020 eruption. (a) Number of shallow volcanotectonic earthquakes per hour. Insets: aerial photographs taken on 3 April (Imaz Press Réunion) and 5 April (SAG-PGHM), and from the "Cascades" OVPF ground webcam on 6 April. (b) Average amplitudes of the vertical component of the FJS OVPF seismic station, located 1.7 km northwest of the eruptive site, in different frequency bands. The signals are filtered, and the average amplitude is calculated over 1 min. (c) Summit deformation as recorded by a GNSS baseline variation. Inset: location of the baseline. (d) Tilt (in black) and air temperature (in red) recorded on the north–south direction on the FLR

station, located 200 m from the eruptive fissure. (e) SO_2 flux measured by the PARN NOVAC station located at 4 km northwest of the eruptive site. (f) Discharge rates (black bars) estimated by the HOTVOLC platform and daily cumulative rainfall (in blue) recorded at the summit by the SFRI OVPF pluviometer. (g) Discharge rates (blue bars) estimated by the MIROVA platform. Heavy cloud cover prevented accurate estimate of discharge rates during much of the eruption, during which absolute values and trends are unreliable due to variable degrees of cloud cover (After Peltier et al., 2020).

References

Benito-Saz, M. A., Sigmundsson, F., Charco, M., Hooper, A., and Parks, M. (2019). Magma flow rates and temporal evolution of the 2012–2014 post-eruptive intrusions at el hierro, canary islands. *Journal of Geophysical Research: Solid Earth*, 124(12):12576–12592.

Gaddes ME, Hooper A, Bagnardi M. (2019). Using Machine Learning to Automatically Detect Volcanic Unrest in a Time Series of Interferograms. Journal of Geophysical Research: Solid Earth. 124(11), pp. 12304-12322

Heiligmann, M., Stix, J., Williams-Jones, G., Lollar, B. S., & Garzón, V. G. (1997). Distal degassing of radon and carbon dioxide on Galeras volcano, Colombia. *Journal of Volcanology and Geothermal Research*, *77*(1-4), 267-283.

Hooper, A., Segall, P., & Zebker, H. (2007). Persistent scatterer interferometric synthetic aperture radar for crustal deformation analysis, with application to Volcán Alcedo, Galápagos. *Journal of Geophysical Research: Solid Earth*, *112*(B7).

Juncu, D., Árnadóttir, T., Hooper, A., and Gunnarsson, G. (2017). Anthropogenic and natural ground deformation in the Hengill geothermal area, Iceland. *Journal of Geophysical Research: Solid Earth*, 122(1):692–709.

Lazecký M, Spaans K, González PJ, Maghsoudi Y, Morishita Y, Albino F, Elliott J, Greenall N, Hatton E, Hooper A, Juncu D, McDougall A, Walters RJ, Watson CS, Weiss JR, Wright TJ. (2020). LiCSAR: An Automatic InSAR Tool for Measuring and Monitoring Tectonic and Volcanic Activity. Remote Sensing. 12(15)

Morishita Y, Lazecky M, Wright TJ, Weiss JR, Elliott JR, Hooper A. (2020). LiCSBAS: An Open-Source InSAR Time Series Analysis Package Integrated with the LiCSAR Automated Sentinel-1 InSAR Processor. Remote Sensing. 12(3).

Padilla, G. D., Hernández, P. A., Padrón, E., Barrancos, J., Pérez, N. M., Melián, G., ... & Hernández, I. (2013). Soil gas radon emissions and volcanic activity at El Hierro (Canary Islands): The 2011-2012 submarine eruption. *Geochemistry, Geophysics, Geosystems*, *14*(2), 432-447.

Peltier, A., V. Ferrazzini, A. Di Muro, P. Kowalski, N. Villeneuve, N. Richter, O. Chevrel, J. L. Froger, A. Hrysiewicz, M. Gouhier, et al. (2020). Volcano Crisis Management at Piton de la Fournaise (La Réunion) during the COVID-19 Lockdown, Seismol. Res. Lett., 1–15, doi: 10.1785/0220200212.

Sæmundsson, K., Sigurgeirsson, M. Á., & Friðleifsson, G. Ó. (2020). Geology and structure of the Reykjanes volcanic system, Iceland. *Journal of Volcanology and Geothermal Research*, *391*, 106501.

Shreve, T., R. Grandin, D. Smittarello, V. Cayol, V. Pinel, Y. Morishita (2021), What triggers caldera ring-fault subsidence at Ambrym volcano? Insights from the 2015 dike intrusion and eruption, J. Geophys. Res.*: Solid Earth*, e2020JB020277.

Sigmundsson, F., Pinel, V., Grapenthin, R., Hooper, A., Halldórsson, S.A., Einarsson, P., Ófeigsson, B. G., Heimisson, E. R., Jónsdóttir, K., Gudmundsson, M.T., Vogfjörð, K., Parks, M., Li, S., Drouin, V., Geirsson, H., Dumont, S., Fridriksdottir, H. M., Gudmundsson, G. B., Wright, T., Tadashi Yamasaki, T. (**2020**), Unexpected large eruptions from buoyant magma bodies within viscoelastic crust, *Nature Communications*, 11, 2403.

Smittarello, D., Cayol, V., Pinel, V., Peltier, A., Froger, J-L., & Ferrazzini, V.. Magma propagation at Piton de la Fournaise from joint inversion of InSAR and GNSS. *Journal of Geophysical Research*, 124, 1361– 1387, https://doi.org/10.1029/2018JB016856, 2019a.

Smittarello, D., V. Cayol, V. Pinel, J.-L. Froger, A. Peltier, Q. Dumont, Combining InSAR and GNSS to track magma transport at basaltic volcanoes, Invited publication at *Remote sensing*, vol.11, p.2236, DOI:*10.3390/rs11192236*, 2019b.